Sciencexpress Reports

The weakening summer circulation in the Northern Hemisphere mid-latitudes

Dim Coumou,[1]* Jascha Lehmann,[1,2] Johanna Beckmann[1,2]

[1]Potsdam Institute for Climate Impact Research, Earth System Analysis, 14412 Potsdam, Germany. [2]University of Potsdam, Potsdam, Germany.

*Corresponding author. E-mail: coumou@pik-potsdam.de

Rapid warming in the Arctic could influence mid-latitude circulation by reducing the poleward temperature gradient. The largest changes are generally expected in autumn or winter but whether significant changes have occurred is debated. Here we report significant weakening of summer circulation detected in three key dynamical quantities: (i) the zonal-mean zonal wind, (ii) the eddy kinetic energy (EKE) and (iii) the amplitude of fast-moving Rossby waves. Weakening of the zonal wind is explained by a reduction in poleward temperature gradient. Changes in Rossby waves and EKE are consistent with regression analyses of climate model projections and changes over the seasonal cycle. Monthly heat extremes are associated with low EKE and thus the observed weakening might have contributed to more persistent heat waves in recent summers.

Enhanced warming in the Arctic could change circulation patterns in the mid-latitudes by reducing the pole-to-mid-latitude thermal gradient (*1–3*). This hypothesis, which was first proposed in the 1970s based on model experiments (*4*, *5*), has recently received considerable attention due to rapid observed warming in the Arctic (*6–9*), associated with a decline in sea-ice and other factors (*1*, *3*, *10*).

Most studies addressing the link between Arctic change and mid-latitude weather have focused on winter circulation. The extra heat stored in the ocean owing to sea-ice loss is released into the atmosphere by late autumn or early winter when air temperatures drop below sea surface temperatures. Consequently, the largest absolute increases in Arctic geopotential height have been detected for autumn and winter (*6*), consistent with climate-model simulations (*11*). Autumn has, at least in the western half of the hemisphere, also seen a reduction in the zonal-mean flow (*6*, *12*). This might cause a slowdown in wave propagation (*6*), but the results are sensitive to the exact metrics used to describe waves (*12*, *13*). Thus, whether observed changes in geopotential height have affected mid-latitude Rossby waves remains disputed (*6*, *12–14*).

Here we study changes in mid-latitude circulation in boreal summer instead. Though the oceanic heat flux is smaller in this season (*11*), Arctic amplification has reduced the pole-to-mid-latitude temperature gradient (*1*) and Arctic geopotential heights have increased (*6*). These changes are likely related to the earlier loss of snow cover over land and increased Arctic sea-surface temperatures where sea-ice has been lost (*7*). In recent summers, mid-latitude circulation has been dominated by a negative Arctic Oscillation index, i.e., anomalously small pressure differences between mid- and high-latitudes (*7*, *15–17*). Moreover, several recent heat waves, like in Russia in 2010, were associated with persistent hemispheric circulation patterns (*15*, *16*, *18*).

Generally, the large-scale mid-latitude atmosphere dynamics [supplementary materials (SM) text S4] are characterized by (i) fast-traveling free Rossby waves (the so called synoptic transients) with zonal wave numbers typically larger than 6, and (ii) quasi-stationary Rossby waves with normally smaller wave numbers as a response to quasi-stationary diabatic and orographic forcing (*15*, *19–21*). We focus on the first. These waves are associated with synoptic-scale cyclones (storms) and anticyclones (high-pressure systems) which form the storm track regions in the mid-latitudes. They have a relatively fast phase-velocity (i.e., eastward propagation) and cause weather variability on timescales of less than a week. Typically, the intensity of synoptic-scale wave (or eddy) activity is estimated by applying a 2.5-6 day bandpass filter to high-resolution wind field data (*22–24*). This way the total eddy kinetic energy (EKE) is extracted which is a measure for the interplay between intensity and frequency of high and low pressure systems associated with fast-traveling Rossby waves. Due to the quasi-stationary nature of thermally and orographically forced waves, as analyzed in related studies (*15*, *16*, *25*, *26*), they have lower frequencies and are thus excluded from our EKE computations (SM text S4).

We calculate EKE in the Northern Hemisphere from daily ERA-Interim wind fields (*27*) using a 2.5-6 day bandpass filter [see (*23*, *24*, *28*)]. We limit our analysis to the satellite covered period (post-1979) to minimize the effects of changes in observing system (SM text S2). The 1979-2013 period has seen a steady decline in summertime EKE (Fig. 1A). This decline is statistically significant at the 1%-level and observed at all pressure levels with the strongest relative changes in the lower to mid-troposphere (figs. S1 to S4 and table S1). Moreover, it occurs over the full hemisphere and over all relevant latitudes (fig. S5). The observed changes are thus not due to a North-South shift of storm tracks but due to a spatially homogeneous weakening. Other reanalysis products give similar results (figs. S6 to S11). For the other seasons, trends in EKE are also downwards but none are significant (figs. S12 to S17).

The decline in summer EKE is accompanied by a long-

term decline in the zonal-mean zonal wind (U, Fig. 1B). Again this weakening of the zonal flow is seen at all altitudes and in different reanalysis products (figs. S1 to S4 and S6 to S10). The long-term weakening of the zonal flow is consistent with the decline in the pole-to-mid-latitude thermal gradient. This is shown by the downward trend of similar magnitude in thermal wind U_T (Fig. 1C), which depends on changes in the temperature gradient only (eq. S2).

While the relative decrease in EKE has been by 8-15% (depending on pressure level) over the 35 year period, the zonal flow weakened by only 4-6% (table S1). A similar relationship between changes in EKE and zonal flow is seen in future projections of CMIP5 climate models. Under a high-emission scenario, summer EKE declines, primarily due to decreased vertical wind shear associated with weakening of the zonal-mean flow (*24*). This projected reduction in EKE is spatially homogeneous, similar to the observed changes. Regression analysis of future changes in EKE and in zonal flow for individual CMIP5 models reveals a significant linear relationship (Fig. 2). The regression slope of ~1.4 indicates that a reduction in U is associated with a more pronounced reduction in EKE. This is seen at all pressure levels with the regression slope increasing with altitude (fig. S18). Increased static stability plays a role as well (*24*, *29*), which explains why the linear regression crosses the y-axis at negative values: Even for zero change in U, increased static stability in a warmer climate causes EKE to decline. The observed relative changes in U and EKE over the past 35 years map reasonably well on the regression of projected future changes (Fig. 2).

The pronounced weakening in EKE should also be reflected in changed wave characteristics. To test this, we apply spectral analysis to the North-South wind component v in daily wind field data and calculate amplitude (A_v), phase speed and period for wave numbers 1-15 (SM text S1.1). This way, fast-moving and quasi-stationary waves are not explicitly separated (as in EKE by using bandpass filtering) but since we use daily data, mean wave amplitudes will be dominated by fast-moving waves (SM text S4). The results are therefore comparable with EKE. We determine the wave quantities for the North-South wind component v averaged over 35°N-70°N and A_v thus reflects wind speeds with units of m/s.

The amplitude of all wave numbers except 7 have declined, with significant reductions in wave 1, 3, 4, 6, 10 and in the mean amplitude of all waves. These changes are robust, detected in ERA-Interim, NCEP-NCAR, and for different pressure levels with the strongest changes in the mid-troposphere (Fig. 3A and fig. S19). This vertical pattern is consistent with the more-pronounced changes in EKE, U (table S1) and poleward temperature gradient (*1*) in the lower troposphere. The mean amplitude declined by -5% over 1979-2013 (Fig. 3A), similar to the relative reduction in U (fig. S1B). This is consistent with the seasonal correlation of these quantities (Fig. 3B) which shows that – to a first order – daily anomalies in mean A_v scale with those in U. This positive correlation is expected as daily wind fields, and thus A_v, will be dominated by transient eddies because their kinetic energy is nearly an order of magnitude larger than that of quasi-stationary waves (*30*). Transient eddies are not only forced by the zonal flow via vertical shear (and thus baroclinicity) but can also accelerate it via the eddy-driven jet (*1*, *31*), explaining the positive correlation between U and A_v (SM text S4). The reduction of -5% in mean wind speed (A_v) implies a –10% reduction in kinetic energy, which is in good agreement with the bandpass filtered results.

Wave 10 has seen a significant reduction in both amplitude and phase speed (Fig. 3A), which dropped respectively by –11% and –20% over the 1979–2013 period, with both negative trends acting to reduce EKE. A reduction in amplitude means lower wind speeds associated with weaker high and low pressure synoptic weather systems and thus lower EKE. A reduced phase speed implies more persistent synoptic weather systems and fewer of them over the full season. The probability-density distribution of wave period shows that wave periods in the EKE-relevant range (2.5-6 days) are dominated by wave 10 (fig. S21). During roughly half of all summer days, wave 10 had a wave period within this range. This suggests that the reduction in amplitude and phase speed of wave 10 contributed substantially to the reduction in EKE.

Summer EKE declined by 8-15% over the last decades whereas the CMIP5 models project similar changes only by the end of the 21st century under a high-emission scenario (*24*). Either the climate models under-predict dynamical changes, or multi-decadal variability played a role in the observed changes. In the other seasons dynamics weakened as well but, here, significant changes are only detected for the zonal-mean flow in autumn (SM text S3). Though the Arctic has warmed most in winter (*1*), the strongest changes in the meridional temperature gradient within the mid-latitudes occurred in summer, followed by autumn (fig. S17). Therefore U_T and U itself weakened most in those seasons (fig. S17). The smaller year-to-year variability in these seasons (and especially in summer), as compared to winter, improves signal-to-noise ratios making trend-detection possible at an earlier stage (fig. S15). Likewise, variability in summer EKE is only half that of the other seasons (fig. S16B) and hence the signal-to-noise ratio is much larger for summer. In fact, summer EKE has weakened by more than two standard deviations over 1979–2013 (fig. S16C). Therefore, contrary to previous suggestions (*1–3*), the influence of Arctic amplification on mid-latitude weather is unlikely to be limited to autumn and winter only.

In summer, synoptic storms transport moist and cool air from the oceans to the continents bringing relief during periods of oppressive heat. Low cyclone activity over Europe in recent years has led to more persistent weather (*32*, *33*) contributing to prolonged heat waves. Regression analysis between EKE and near-surface temperature for summer

months reveals that over mid-latitude continental regions these quantities are negatively correlated (Fig. 4A). Thus, hot summer months are associated with low EKE (SM text S5). Over most of Eurasia and the U.S., the negative regression slope is significant at the 5%-level. In these storm track affected regions, EKE in the 10% hottest months was only about half its summer climatological value (Fig. 4B and figs. S22 to S24). Low cyclone activity (and thus low EKE) implies that cool maritime air masses become less frequent creating favorable conditions for the build-up of heat and drought over continents. This likely prolongs the duration of blocking weather systems, as for example during the Russian heat wave of 2010 (*18*, *34*). In particular, the record-breaking July temperatures over Moscow were associated with extremely low EKE (Fig. 4B).

Recent studies emphasized the importance of quasi-stationary waves for summer heat extremes (*15*, *16*, *25*, *35*), showing that the frequency of wave-resonance events associated with high-amplitude quasi-stationary waves has increased since the onset of rapid Arctic amplification in 2000 (*16*). Here we show that the amplitude of fast-moving waves has steadily decreased and also the rate in this weakening seems to have increased since 2000 (fig. S25). Both these observations are consistent with more persistent summer weather (SM text S6). Low monthly EKE implies low weather variability within that month indicating persistent weather conditions, consistent with quasi-stationary waves. The long-term reduction in EKE should lead to a reduction in weather variability on short timescales (less than a week), in agreement with the reduced intra-seasonal daily temperature variance observed (*36*) and theoretical arguments (*37*). However, our results show that low EKE is associated with heat extremes on monthly timescales. Therefore, on such longer time scales variability might actually increase due to a reduction in EKE. This seems consistent with Huntingford *et al.* (*38*) who report that the largest increase in inter-annual seasonal temperature variance occurred in the mid-latitude boreal summer. To test this hypothesis, studies are needed which quantify both inter-annual and intra-annual variability on all relevant sub-seasonal timescales.

This study shows that boreal summer circulation has weakened together with a reduction in the pole-to-mid-latitude temperature gradient. This has made weather more persistent and hence favored the occurrence of prolonged heat extremes.

REFERENCES AND NOTES

1. J. Cohen, J. A. Screen, J. C. Furtado, M. Barlow, D. Whittleston, D. Coumou, J. Francis, K. Dethloff, D. Entekhabi, J. Overland, J. Jones, Recent Arctic amplification and extreme mid-latitude weather. *Nat. Geosci.* **7**, 627–637 (2014). doi:10.1038/ngeo2234
2. D. Budikova, Role of Arctic sea ice in global atmospheric circulation: A review. *Global Planet. Change* **68**, 149–163 (2009). doi:10.1016/j.gloplacha.2009.04.001
3. J. E. Walsh, Intensified warming of the Arctic: Causes and impacts on middle latitudes. *Global Planet. Change* **117**, 52–63 (2014). doi:10.1016/j.gloplacha.2014.03.003
4. R. L. Newson, Response of a general circulation model of the atmosphere to removal of the arctic ice-cap. *Nature* **241**, 39–40 (1973). doi:10.1038/241039b0
5. M. Warshaw, R. R. Rapp, An experiment on the sensitivity of a global circulation model. *J. Appl. Meteorol.* **12**, 43–49 (1973). doi:10.1175/1520-0450(1973)012<0043:AEOTSO>2.0.CO;2
6. J. A. Francis, S. J. Vavrus, Evidence linking Arctic amplification to extreme weather in mid-latitudes. *Geophys. Res. Lett.* **39**, L06801 (2012). doi:10.1029/2012GL051000
7. J. E. Overland, J. A. Francis, E. Hanna, M. Wang, The recent shift in early summer Arctic atmospheric circulation. *Geophys. Res. Lett.* **39**, L19804 (2012). doi:10.1029/2012GL053268
8. R. Jaiser, K. Dethloff, D. Handorf, A. Rinke, J. Cohen, Impact of sea ice cover changes on the Northern Hemisphere atmospheric winter circulation. *Tellus, Ser. A, Dyn. Meterol. Oceanogr.* **64**, 1–11 (2012). doi:10.3402/tellusa.v64i0.11595
9. J. L. Cohen, J. C. Furtado, M. A. Barlow, V. A. Alexeev, J. E. Cherry, Arctic warming, increasing snow cover and widespread boreal winter cooling. *Environ. Res. Lett.* **7**, 014007 (2012). doi:10.1088/1748-9326/7/1/014007
10. F. Pithan, T. Mauritsen, *Nat. Geosci.* (2014).
11. J. A. Screen, I. Simmonds, C. Deser, R. Tomas, The atmospheric response to three decades of observed arctic sea ice loss. *J. Clim.* **26**, 1230–1248 (2013). doi:10.1175/JCLI-D-12-00063.1
12. E. A. Barnes, Revisiting the evidence linking Arctic amplification to extreme weather in midlatitudes. *Geophys. Res. Lett.* **40**, 4734–4739 (2013). doi:10.1002/grl.50880
13. J. A. Screen, I. Simmonds, Exploring links between Arctic amplification and mid-latitude weather. *Geophys. Res. Lett.* **40**, 959–964 (2013). doi:10.1002/grl.50174
14. E. Kintisch, Into the maelstrom. *Science* **344**, 250–253 (2014). Medline doi:10.1126/science.344.6181.250
15. V. Petoukhov, S. Rahmstorf, S. Petri, H. J. Schellnhuber, Quasiresonant amplification of planetary waves and recent Northern Hemisphere weather extremes. *Proc. Natl. Acad. Sci. U.S.A.* **110**, 5336–5341 (2013). Medline doi:10.1073/pnas.1222000110
16. D. Coumou, V. Petoukhov, S. Rahmstorf, S. Petri, H. J. Schellnhuber, Quasi-resonant circulation regimes and hemispheric synchronization of extreme weather in boreal summer. *Proc. Natl. Acad. Sci. U.S.A.* **111**, 12331–12336 (2014). Medline doi:10.1073/pnas.1412797111
17. J. A. Screen, Influence of Arctic sea ice on European summer precipitation. *Environ. Res. Lett.* **8**, 044015 (2013). doi:10.1088/1748-9326/8/4/044015
18. S. Schubert, H. Wang, M. Suarez, Warm season subseasonal variability and climate extremes in the Northern Hemisphere: The role of stationary Rossby Waves. *J. Clim.* **24**, 4773–4792 (2011). doi:10.1175/JCLI-D-10-05035.1
19. J. Pedlosky, *Geophysical Fluid Dynamics* (Springer, New York, 1979).
20. K. Fraedrich, H. Böttger, A wavenumber-frequency analysis of the 500 mb geopotential at 50°N. *J. Atmos. Sci.* **35**, 745–750 (1978). doi:10.1175/1520-0469(1978)035<0745:AWFAOT>2.0.CO;2
21. G. J. Boer, T. G. Shepherd, Large-scale two-dimensional turbulence in the atmosphere. *J. Atmos. Sci.* **40**, 164–184 (1983). doi:10.1175/1520-0469(1983)040<0164:LSTDTI>2.0.CO;2
22. M. Blackmon, A climatological spectral study of the 500 mb geopotential height of the Northern Hemisphere. *J. Atmos. Sci.* **33**, 1607–1623 (1976). doi:10.1175/1520-0469(1976)033<1607:ACSSOT>2.0.CO;2
23. D. Coumou, V. Petoukhov, A. V. Eliseev, Three-dimensional parameterizations of the synoptic scale kinetic energy and momentum flux in the Earth's atmosphere. *Nonlinear Process. Geophys.* **18**, 807–827 (2011). doi:10.5194/npg-18-807-2011
24. J. Lehmann, D. Coumou, K. Frieler, A. V. Eliseev, A. Levermann, Future changes in extratropical storm tracks and baroclinicity under climate change. *Environ. Res. Lett.* **9**, 084002 (2014). doi:10.1088/1748-9326/9/8/084002
25. H. Teng, G. Branstator, H. Wang, G. Meehl, W. M. Washington, Probability of US heat waves affected by a subseasonal planetary wave pattern. *Nat. Geosci.* **6**, 1–6 (2013). doi:10.1038/ngeo1988
26. K. E. Trenberth, J. T. Fasullo, G. Branstator, A. S. Phillips, Seasonal aspects of the recent pause in surface warming. *Nat. Clim. Chang.* **4**, 911–916 (2014). doi:10.1038/nclimate2341
27. D. P. Dee, S. M. Uppala, A. J. Simmons, P. Berrisford, P. Poli, S. Kobayashi, U. Andrae, M. A. Balmaseda, G. Balsamo, P. Bauer, P. Bechtold, A. C. M. Beljaars, L. van de Berg, J. Bidlot, N. Bormann, C. Delsol, R. Dragani, M. Fuentes, A. J. Geer, L. Haimberger, S. B. Healy, H. Hersbach, E. V. Hólm, L. Isaksen, P. Kållberg, M. Köhler, M. Matricardi, A. P. McNally, B. M. Monge-Sanz, J.-J. Morcrette, B.-K.

Park, C. Peubey, P. de Rosnay, C. Tavolato, J.-N. Thépaut, F. Vitart, The ERA-Interim reanalysis: Configuration and performance of the data assimilation system. *Q. J. R. Meteorol. Soc.* **137**, 553–597 (2011). doi:10.1002/qj.828
28. M. Murakami, Large-scale aspects of deep convective activity over the GATE area. *Mon. Weather Rev.* **107**, 994–1013 (1979). doi:10.1175/1520-0493(1979)107<0994:LSAODC>2.0.CO;2
29. J. Lu, G. Chen, D. M. W. Frierson, Response of the zonal mean atmospheric circulation to El Niño versus global warming. *J. Clim.* **21**, 5835–5851 (2008). doi:10.1175/2008JCLI2200.1
30. J. P. Peixoto, A. H. Oort, *Physics of Climate*
31. T. Woollings, M. Blackburn, The North Atlantic jet stream under climate change and its relation to the NAO and EA patterns. *J. Clim.* **25**, 886–902 (2012). doi:10.1175/JCLI-D-11-00087.1
32. J. Kyselý, R. Huth, Changes in atmospheric circulation over Europe detected by objective and subjective methods. *Theor. Appl. Climatol.* **85**, 19–36 (2005). doi:10.1007/s00704-005-0164-x
33. J. Kyselý, Influence of the persistence of circulation patterns on warm and cold temperature anomalies in Europe: Analysis over the 20th century. *Global Planet. Change* **62**, 147–163 (2008). doi:10.1016/j.gloplacha.2008.01.003
34. R. Dole, M. Hoerling, J. Perlwitz, J. Eischeid, P. Pegion, T. Zhang, X.-W. Quan, T. Xu, D. Murray, Was there a basis for anticipating the 2010 Russian heat wave? *Geophys. Res. Lett.* **38**, L06702 (2011). doi:10.1029/2010GL046582
35. J. A. Screen, I. Simmonds, Amplified mid-latitude planetary waves favour particular regional weather extremes. *Nat. Clim. Chang.* **4**, 704–709 (2014). doi:10.1038/nclimate2271
36. J. A. Screen, Arctic amplification decreases temperature variance in northern mid- to high-latitudes. *Nat. Clim. Chang.* **4**, 577–582 (2014). doi:10.1038/nclimate2268
37. T. Schneider, T. Bischoff, H. Plotka, *J. Clim.* (2014).
38. C. Huntingford, P. D. Jones, V. N. Livina, T. M. Lenton, P. M. Cox, No increase in global temperature variability despite changing regional patterns. *Nature* **500**, 327–330 (2013). Medline doi:10.1038/nature12310

ACKNOWLEDGMENTS

We thank the CMIP5 climate modeling groups and ECMWF and NCEP-NCAR for making their model and reanalysis data available. Comments by three anonymous reviewers, S. Rahmstorf, and P. Eickemeier have considerably improved the manuscript. Data presented in this manuscript will be archived for at least 10 years by the Potsdam Institute for Climate Impact Research. The work was supported by the German research Foundation (CO994/2-1) and the German Federal Ministry of Education and Research (01LN1304A). D.C. designed the research; D.C., .J.L., and J.B. performed the analysis; and D.C., J.L., and J.B. wrote the manuscript.

SUPPLEMENTARY MATERIALS

www.sciencemag.org/cgi/content/full/science.1261768/DC1
Text S1 to S6
Figs. S1 to S25
Table S1
References
Data Deposition

26 September 2014; accepted 26 February 2015
Published online 12 March 2015; 10.1126/science.1261768

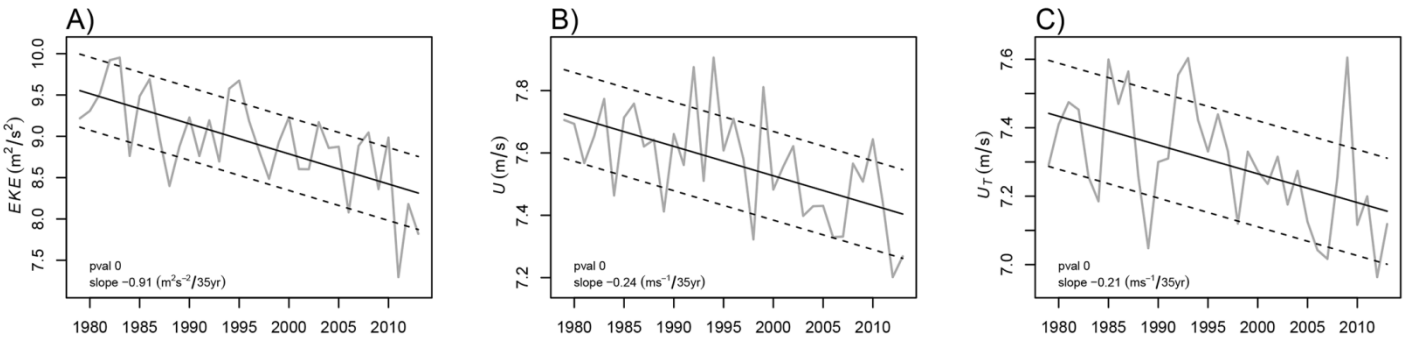

Fig. 1. Weakening summer circulation in the mid-latitudes. Absolute changes in (**A**) eddy kinetic energy EKE, (**B**) zonal wind U, and (**C**) thermal wind U_T over 1979–2013 in summer (JJA). Variables are calculated at 500 mb and averaged over 35°N-70°N and all longitudes with gray lines plotting observations, solid black lines the linear trend and dashed black lines the +/− 1 residual standard error range. Slope and P values for the trend estimates are given in the panels.

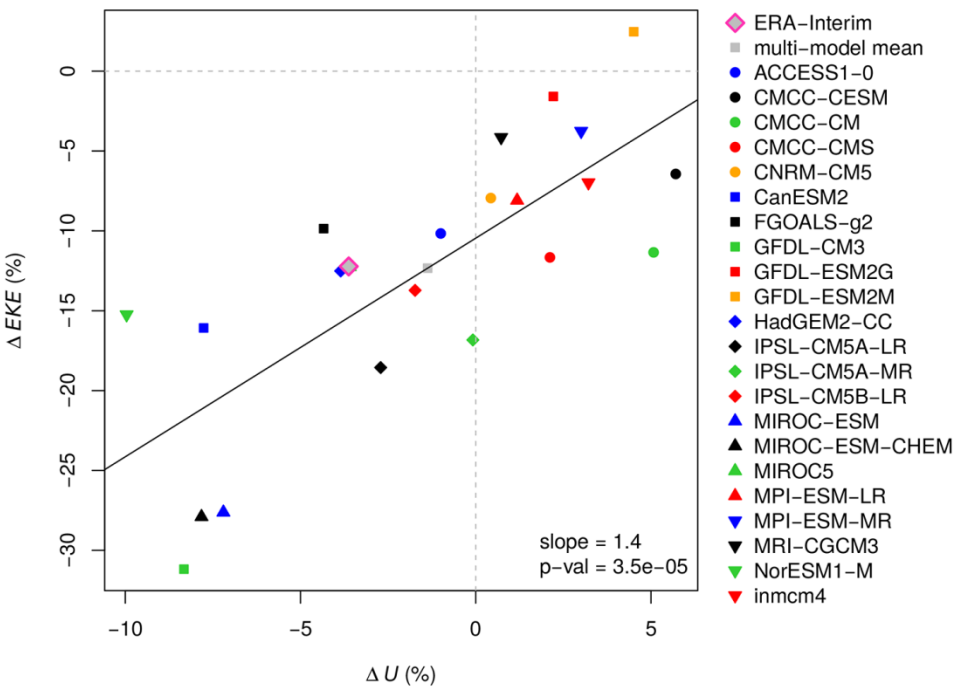

Fig. 2. Relationship between relative changes in EKE and *U* in climate model projections. Percentage change in future (2081–2100, under scenario RCP8.5) relative to 1981–2000 for individual CMIP5 climate models. Both quantities are averaged over 35°N-70°N, all longitudes and over 850 mb-250 mb (mass-weighted). The solid black line shows the linear fit with slope and *P* value given in the panel. Relative changes in EKE and *U* in the ERA-Interim data are given for the 1979–2013 period.

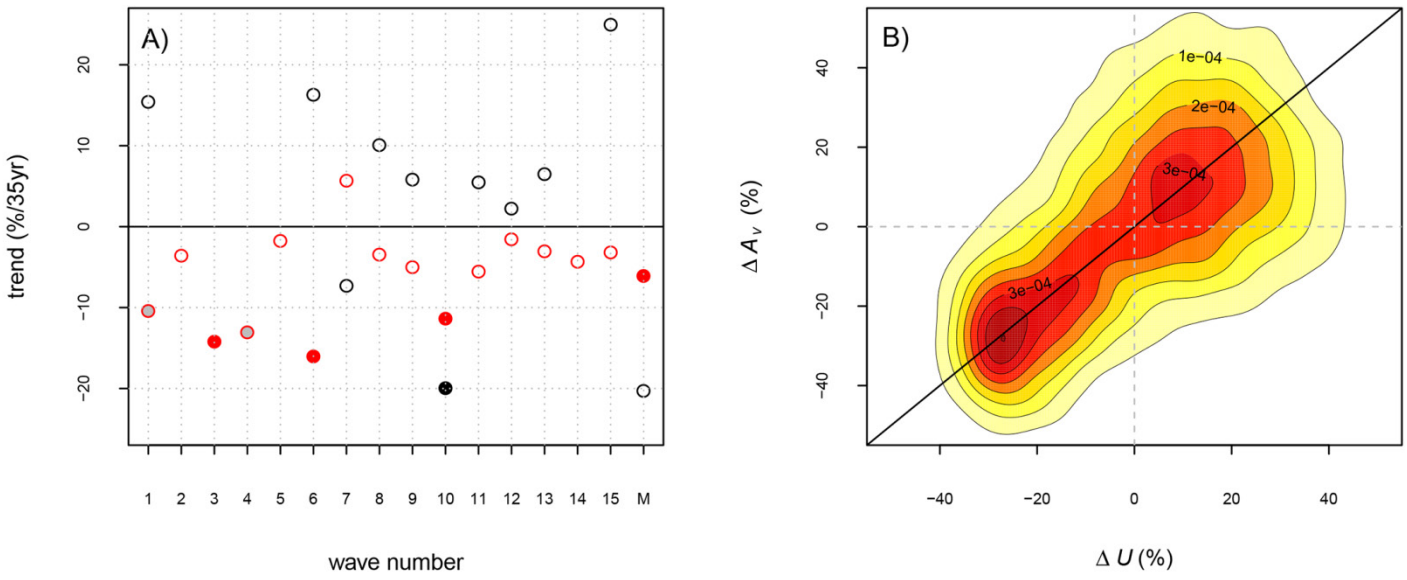

Fig. 3. (**A**) Trends in planetary wave amplitudes (A_v, red) and phase speed (black) at 500 mb in summer for wave numbers 1-15 and for the mean of all waves (M) in units of percentage change per 35 years, i.e., the period 1979–2013. Solid circles indicate 5% statistical significance, gray-filled circles 10% statistical significance and open circles are not significant. (**B**) 2D probability density distribution of daily deviations (in percentage change of their annual-mean climatological values) of the zonal flow and the mean amplitude of waves 1-15. The bisecting line is shown in black.

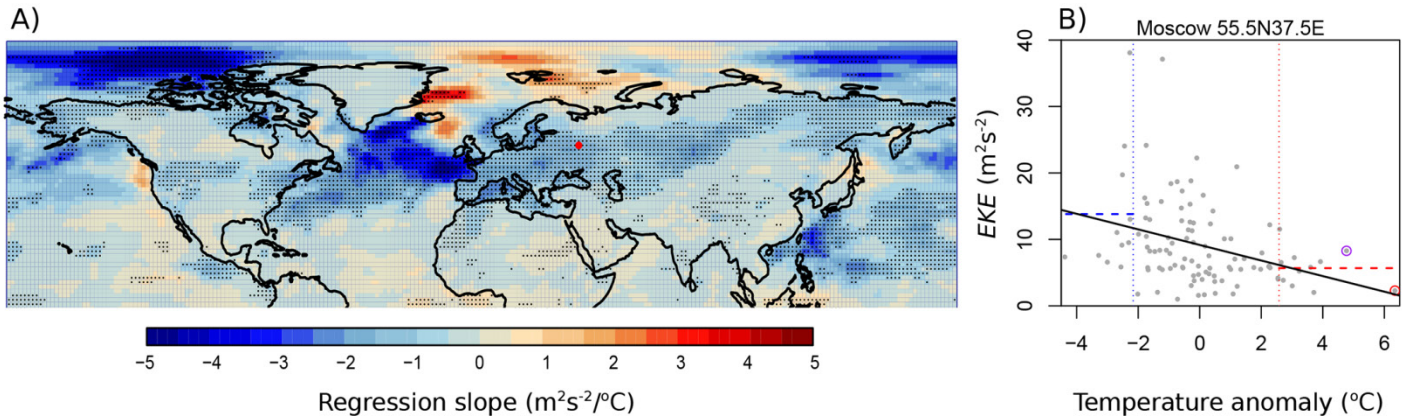

Fig. 4. Regression analysis between EKE and near-surface temperature during summer months (June, July, August). (**A**) Slope of the regression analysis. Both variables were linearly detrended and stippling indicates significance at the 5%-level. (**B**) EKE plotted against near-surface temperature anomaly for Moscow [red dot in (A)] for individual summer months, showing that the 10% coldest summer months (left of the vertical blue dotted line) have a substantially higher EKE (14 m^2/s^2, i.e., the horizontal blue dashed line) and the 10% warmest months (right of the vertical red dotted line) a substantially lower EKE (5.7 m^2/s^2, i.e., the horizontal red dashed line). Red and purple circles indicate, respectively, July and August 2010.